Epidemic spreading on random surfer networks with infected avoidance strategy*

Yun Feng(冯运)[1], Li Ding(丁李)[1,†], Yun-Han Huang(黄蕴涵)[1], and Zhi-Hong Guan(关治洪)[2]

[1] *Department of Automation, School of Power and Mechanical Engineering, Wuhan University, Wuhan* 430072, *China.*
[2] *College of Automation, Huazhong University of Science and Technology, Wuhan* 430074, *China*

(Received 17 June 2016; revised manuscript received 18 August 2016; published online 25 October 2016)

In this paper, we study epidemic spreading on random surfer networks with infected avoidance (IA) strategy. In particular, we consider that susceptible individuals' moving direction angles are affected by the current location information received from infected individuals through a directed information network. The model is mainly analyzed by discrete-time numerical simulations. The results indicate that the IA strategy can restrain epidemic spreading effectively. However, when long-distance jumps of individuals exist, the IA strategy's effectiveness on restraining epidemic spreading is heavily reduced. Finally, it is found that the influence of the noises from information transferring process on epidemic spreading is indistinctive.

Keywords: epidemic spreading, SIS model, random surfer networks

PACS: 89.75.Fb, 87.23.Ge, 89.75.–k, 89.75.Hc **DOI:** 10.1088/1674-1056/25/12/128903

1. Introduction

In recent years, an increasing amount of attention has been paid to epidemics spreading over complex networks. One of the well-studied problems is to investigate the transmission behavior of the disease over networks. In most of the literature dealing with the epidemic spreading behavior, the topology structure of the underlying network is assumed to be static.[1–10] However, in practice, the relations between individuals are unlikely to keep unchanged all the time, the movements of individuals cause a dynamic topology structure. In fact, some recent study results indicate that the mobility of individuals can play a significant role in the epidemic spreading process.[11–19] For example, a dynamical network consisting of a time-evolving wiring of interactions among a group of random walkers is introduced to model the spread of an infectious disease in a population of mobile individuals in Ref. [20]. In Ref. [21], a model of mobile agents is proposed to study the epidemic spreading in communities with different densities of agents, which aims at simulating the realistic situation of multiple cities.

In the above work, the movements of individuals are random, which are independent of their current health statuses. However, in real life, it is more reasonable that a susceptible individual tends to move away from its infected neighbors to prevent itself from being infected. Besides, individuals can transfer information about their health statuses and locations to others through the Internet or mobile phone. Susceptible individuals tend to avoid physical contact with infected neighbors whose location information can be received. Motivated by the above considerations, we consider the problems that susceptible individuals can receive current location information from infected neighbors and their moving directions are affected by the received information. However, the infected individuals' moving directions are not subjected to the influence of others. The network in which location information is transferred is set to be a directed information network. More precisely, susceptible individuals can receive location information of infected neighbors, but not vice versa. According to the directed information network, we construct a novel model of epidemic spreading on random surfer networks with Infected Avoidance (IA) strategy. Noises are considered in our model as they commonly exist in the information transferring process. Besides, like in Ref. [20], long-distance jumps are also considered. The model is mainly analyzed by discrete-time numerical simulations.

The main contributions of this paper are given as follows. Firstly, we establish a novel epidemic spreading model based on random surfer networks which considers the IA strategy. The network consists of two layers: one is the physical contact network, and the other is the directed information network. The IA strategy describes the influence of the information network on the physical contact network. The model is analyzed by both theoretical analysis and numerical simulations. Comparing our model with classical epidemic spreading model on random surfer networks, it is found that the IA strategy can control the epidemic outbreak significantly by increasing the

*Project supported in part by the National Natural Science Foundation of China (Grant Nos. 61403284, 61272114, 61673303, and 61672112) and the Marine Renewable Energy Special Fund Project of the State Oceanic Administration of China (Grant No. GHME2013JS01).

†Corresponding author. E-mail: liding@whu.edu.cn

© 2016 Chinese Physical Society and IOP Publishing Ltd

epidemic threshold and reducing the steady-state disease density. When individuals have certain probability to travel to far places within a short period, the effectiveness of IA strategy is heavily reduced. After that, we investigate the influence of the noises on epidemic spreading which commonly exist in the information transferring process. The results indicate that the influence is indistinctive.

The rest of this paper is organized as follows. In Section 2, a novel epidemic spreading model with IA strategy is established. In Section 3, discrete-time simulation results are presented. Finally, we draw some conclusions from the present study in this paper in Section 4.

2. Model

We consider N individuals uniformly distributed in a two-dimensional (2D) space. Each individual has two states: susceptible (S) and infected (I). The spreading process of the epidemic can be summarized as follows. Firstly a contact radius r_c is defined such that each individual has physical contacts at a given time with only those individuals located within a neighborhood of radius r_c. Susceptible individuals have the probability β to be infected by infected individuals through physical contacts in each step. Therefore, the probability that an individual is infected in each step is

$$p_{\inf} = 1-(1-\beta)^{I_{r_c}},$$

where I_{r_c} is the number of infected individuals within a neighborhood of radius r_c. Meanwhile, infected individuals can be cured with the constant probability γ in each step.

2.1. Epidemic spreading model

Based on the above descriptions, the epidemic spreading process can be obtained by

$$p_i(t+1) = \left(1-\prod_{j=1}^{N}(1-\beta p_j(t)a_{ij}(t))\right)(1-p_i(t)) + (1-\gamma)p_i(t), \tag{1}$$

where $p_i(t)$ denotes the probability that individual i is infected at step t and $a_{ij}(t)$ denotes the weight of link between individual i and j at step t.

Remark 1 When $\beta p_j(t)a_{ij}(t) \ll 1$, we have the approximation that

$$1-\prod_{j=1}^{N}(1-\beta p_j(t)a_{ij}(t)) \approx \beta\sum_{j=1}^{N} p_j(t)a_{ij}(t).$$

Thus

$$p_i(t+1) = \beta\sum_{j=1}^{N} p_j(t)a_{ij}(t)+(1-\gamma)p_i(t). \tag{2}$$

Also, equation (2) can be written in the compact form as

$$P(t+1) = ((1-\gamma)I+\beta A(t))P(t), \tag{3}$$

where

$$I = \mathrm{diag}\,(1,1,\ldots,1) \in \Re^{N\times N},$$
$$P(t) = (p_1(t),p_2(t),\ldots,p_N(t)) \in \Re^{N\times 1}.$$

Here $A(t)$ denotes the adjacent matrix of the physical contact network at step t. When $A(t)$ is a constant matrix A, the epidemic spreading threshold λ_c is

$$\lambda_c = \frac{1}{\lambda_{1,A}}$$

in Ref. [22], where $\lambda_{1,A}$ is the largest eigenvalue of A.

At the equilibrium point, we have that $P(t) = P(t+1)$ in Eq. (3). According to Eq. (3), the equilibrium point satisfies either

$$P(t) = (0,0,\ldots,0) \in \Re^{N\times 1}$$

or

$$\langle k\rangle(t) = \frac{\gamma}{\beta},$$

where $\langle k\rangle(t)$ denotes the mean degree of all individuals at step t.

2.2. Random surfer model

The location of the ith individual at step t is denoted as $(x_i(t),y_i(t))$ and the velocity modulus of which is denoted by $v_i(t)$. The motion process can be obtained by

$$\begin{cases} x_i(t+1) = x_i(t)+v_i(t)\cos\theta_i(t), \\ y_i(t+1) = y_i(t)+v_i(t)\sin\theta_i(t), \end{cases} \tag{4}$$

where $\theta_i(t)$ is the direction angle of individual i at step t. Like in Ref. [19], we consider that individuals may perform long-distance jumps, a parameter p_{jump} is defined to quantify the probability that each individual performs long-distance jumps. Therefore, we have

$$\begin{cases} \mathrm{prob}\,\{v_i(t) = v\} = 1-p_{\mathrm{jump}}, \\ \mathrm{prob}\,\{v_i(t) = v_{\mathrm{jump}}\} = p_{\mathrm{jump}}, \end{cases} \tag{5}$$

where v_{jump} is the velocity modulus of individuals which perform long-distance jumps. We consider all individuals performing long-distance jumps with random direction angles in the interval $[-\pi,\pi]$ with uniform probability.

In our model, two layers of network are considered: one is the physical contact network and the other is the directed information network. The adjacent matrix of the physical contact network at step t is obtained by

$$a_{ij}(t) = \begin{cases} 1, & \text{for } \left\|l_i(t)-l_j(t)\right\|_2 \le r_c, \\ 0, & \text{for } \left\|l_i(t)-l_j(t)\right\|_2 > r_c \text{ or } i=j. \end{cases} \tag{6}$$

It indicates that individuals have physical contacts only when the distance between them is smaller than r_c. In Eq. (6), the definition of $a_{ij}(t)$ when $i = j$ is included.

The adjacent matrix of the directed information network at step t is denoted by $B(t)$. We define that $B(t)$ is determined by the locations of individuals and their physical states at step t. More precisely, a sensing radius r_s is defined, such that each susceptible individual can receive location information from those infected individuals located within a neighborhood of radius r_s, but not vice versa. Therefore, $B(t)$ is obtained by

$$b_{ij}(t) = \begin{cases} 1, & \text{for } \|l_i(t) - l_j(t)\|_2 \le r_s \\ & \text{and } p_i(t) = 0 \text{ and } p_j(t) = 1, \\ 0, & \text{otherwise}, \end{cases} \tag{7}$$

when $i = j$, we have $b_{ij}(t) = 0$. The $b_{ij}(t) = 1$ indicates that the individual i can receive the location information from its infected neighbor j. An IA strategy is introduced by adjusting the direction angles of susceptible individuals. Each susceptible individual tends to avoid physical contacts with infected neighbors by adjusting its moving direction away from them.

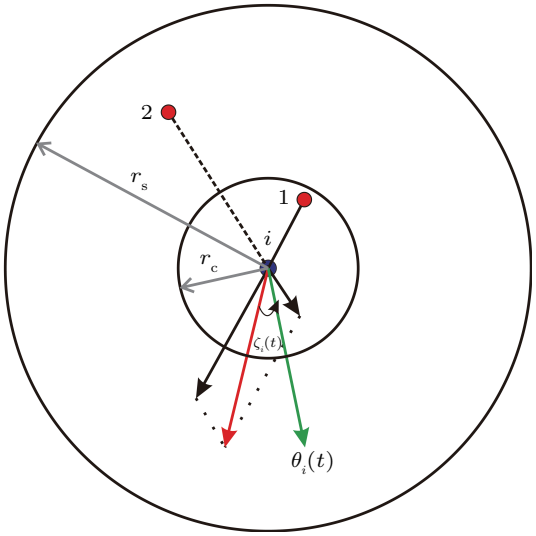


Fig. 1. (color online) An illustrate example of the IA strategy.

Figure 1 shows an example of the IA strategy we considered. The blue node in the center denotes a susceptible individual i while the two red nodes represent the infected individuals. Because $\|l_i - l_1\|_2 < r_s$ and $\|l_i - l_2\|_2 < r_s$, we have $b_{i1} = 1$ and $b_{i2} = 1$ according to Eq. (7). Therefore, the individual i can receive location information from both individuals 1 and 2. The individual i tends to avoid being infected by individuals 1 and 2: this kind of trend can be regarded as a resultant force of both individuals, indicated by the red arrow in the figure. The $\theta_i(t)$ denotes the direction angle under the influence of both infected individuals within the sensing circle r_s and noises in the information transferring process. In the illustrative graph of Fig. 1, we have $r_s > r_c$. However, it is one of the cases we considered. For example, individuals may have communication with others from far distances through the Internet or mobile phone while their physical contact objects are family members, colleagues or classmates. Therefore r_s is larger than r_c in such cases. However, r_s may be smaller than r_c in some cases. Some individuals may travel to far places frequently and have physical contact with strangers. In such cases, r_s is smaller than r_c. Both cases are studied in the following section. The direction angles are updated for all individuals according to

$$\theta_i(t) = \begin{cases} \xi_i(t), & \text{for } b_{ij}(t) = 0, \\ \angle\left(\sum_{j=1}^{I_{r_s}} \dfrac{l_i(t) - l_j(t)}{\|l_i(t) - l_j(t)\|_2^2}\right) + \zeta_i(t), & \text{for } b_{ij}(t) = 1, \end{cases} \tag{8}$$

where $\xi_i(t)$ is an independent variable chosen at each time in the interval $[-\pi, \pi]$ with uniform probability, $l_i(t)$ denotes the location vector of individual i at step t, I_{r_s} is the number of infected individuals within a neighborhood of radius r_s, and $\zeta_i(t)$ denotes the angle deviation caused by the noises in the information transferring process. Without loss of generality, $\zeta_i(t)$ is defined to obey the following Gauss distribution

$$\zeta_i(t) \sim N(\mu, \sigma^2),$$

where $\mu = 0$.

3. Numerical Simulations

The model mentioned in Section 2 is simulated for 500 steps in all the simulations considered in the present paper, which is sufficiently high to ensure that the epidemic reaches a steady-state. The size of the two-dimensional (2D) space is $L \times L$ and the periodic boundary conditions are considered. The density of individuals is defined as $\rho = N/L^2$. The effective infection rate λ is the ratio of infecting probability β to the curing probability γ, thus $\lambda = \beta/\gamma$. For simplicity, the value of γ in all the simulations is define to be 0.1 since it only affects the definition of the timescale of the epidemic spreading. The initial disease density is selected as $i(t_0) = 0.05$ in all simulations.

3.1. Steady-state disease density

It is easily observed from Fig. 2 that with the increase of the contact radius r_c, the steady-state disease density becomes larger. Meanwhile, it decreases with the increase of the sensing radius r_s. Besides, once the contact radius r_c is large enough, the increase of the sensing radius r_s cannot effectively restrain epidemic spreading.

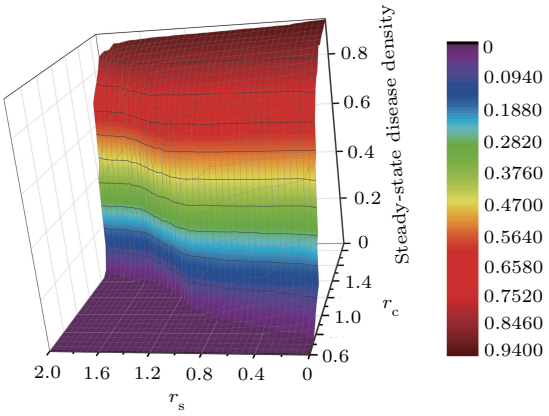


Fig. 2. (color online) Steady-state disease density with respect to contact radius r_c and sensing radius r_s. The parameters of the model are $N = 200$, $L = 20$, $v = 0.05$, $\rho = 0.5$, $\lambda = 2$, $p_{jump} = 0$, $\mu = 0$, and $\sigma = 0$. The results are averaged over 10 runs.

Figure 3 shows the effects of the IA strategy on epidemic spreading. Comparing Fig. 3(a) with Fig. 3(b), it can be concluded that the IA strategy restrains the epidemic from outbreaking significantly. The effectiveness of the IA strategy decrease when r_c is larger than r_s. Besides, epidemic spreading can be effectively restricted when $r_s > r_c$. This phenomenon indicates that the relative size of r_c and r_s affects the effectiveness of the IA strategy.

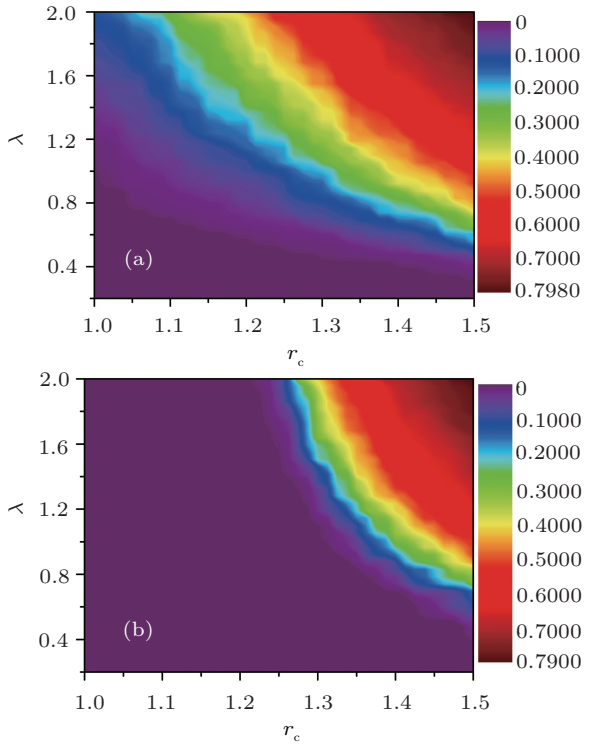


Fig. 3. (color online) Steady-state disease density with respect to contact radius r_c and the effective infection rate λ in the case $r_s = 0$ (a) and $r_s = 1.25$ (b). The parameters of the model are $N = 200$, $L = 20$, $v = 0.05$, $\rho = 0.5$, $\lambda = 2$, $p_{jump} = 0$, $\mu = 0$, and $\sigma = 0$. The results are averaged over 10 runs.

The effects of long-distance jumps on epidemic spreading are studied in Fig. 4. Comparing Fig. 4 with Fig. 3, it can be noticed that the steady-state disease density related to the case with $p_{jump} = 0.1$ is always larger than those related to the case with $p_{jump} = 0$. Therefore, it can be concluded that long-distance jumps cause a larger epidemic spreading scale. Moreover, the IA strategy effectiveness on restraining epidemic spreading is heavily reduced when long-distance jumps exist.

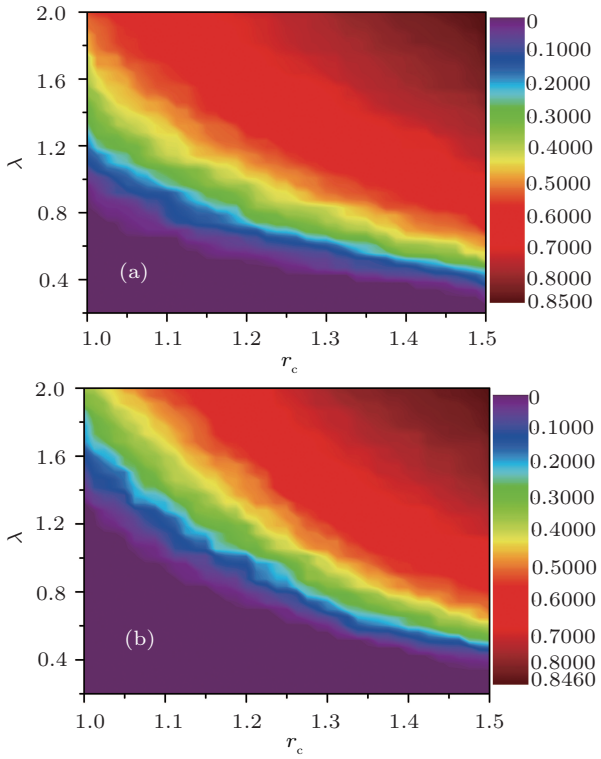


Fig. 4. (color online) Steady-state disease density with respect to contact radius r_c and the effective infection rate λ in the case $r_s = 0$ (a) and $r_s = 1.25$ (b). The parameters of the model are $N = 200$, $L = 20$, $v = 0.05$, $\rho = 0.5$, $\lambda = 2$, $p_{jump} = 0.1$, $v_{jump} = 1$, $\mu = 0$, and $\sigma = 0$. The results are averaged over 10 runs.

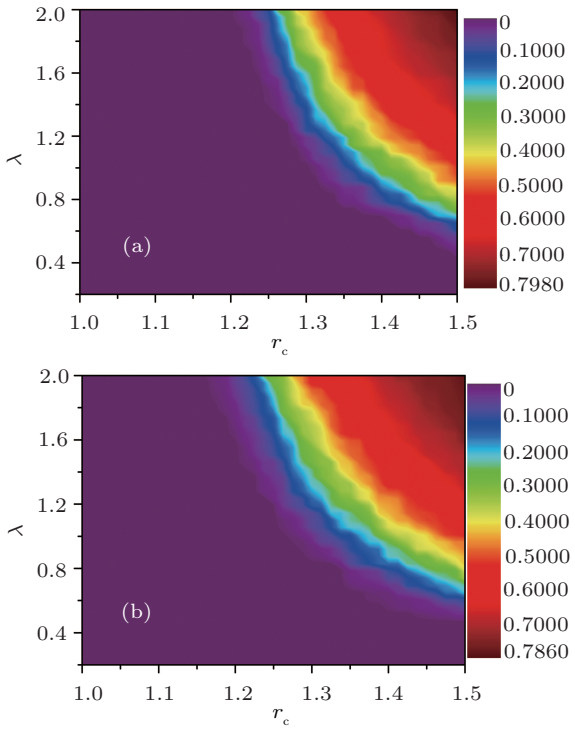


Fig. 5. (color online) Steady-state disease density with respect to contact radius r_c and the effective infection rate λ in the case $\sigma = \pi/6$ (a) and $\sigma = \pi/3$ (b). The parameters of the model are $N = 200$, $L = 20$, $v = 0.05$, $\rho = 0.5$, $r_s = 1.25$, $\lambda = 2$, and $p_{jump} = 0$. The results are averaged over 10 runs.

The behaviors of the model are also characterized with respect to different values of the standard deviation σ of the noise in Fig. 5. It is worthwhile to note that with the value of σ increasing, the effectiveness of the IA strategy on restraining epidemic spreading nearly remains unchanged. This phenomenon validates the effectiveness of the IA strategy in situations with noises.

3.2. Epidemic spreading threshold

The epidemic spreading threshold λ_c, which is the most significant characteristic of our model, is investigated with respect to $p_{\text{jump}} = 0$ and $p_{\text{jump}} = 0.1$ in Fig. 6. It can be easily observed that the IA strategy increases the threshold λ_c significantly, thus restraining the epidemic from outbreaking heavily. However, when the contact radius r_c becomes larger, λ_c approximately equals that without the IA strategy. This indicates that the IA strategy loses effectiveness on restraining the epidemic from outbreaking when $r_c > r_s$. The theoretical result in Ref. [21] with $\lambda_c = 1/\rho\pi r_c^2$ is also plotted for reference, which coincides with the simulation result of $r_s = 0$.

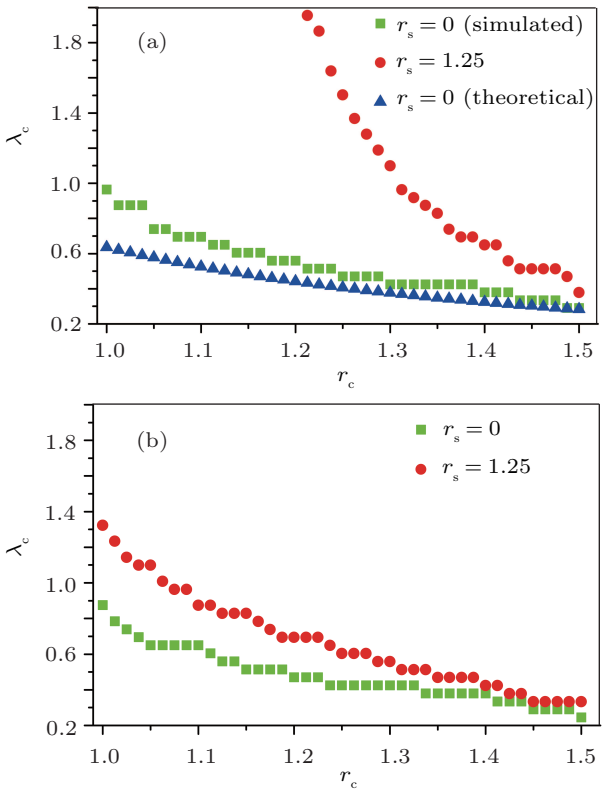


Fig. 6. (color online) Epidemic spreading threshold λ_c with respect to contact radius r_c in the case $p_{\text{jump}} = 0$ (a) and $p_{\text{jump}} = 0.1$ (b). The parameters of the model are $N = 200$, $L = 20$, $v = 0.05$, $v_{\text{jump}} = 1$, $\rho = 0.5$, $\mu = 0$, and $\sigma = 0$. The results are averaged over 10 runs.

When long-distance jumps exist, the IA strategy loses effectiveness heavily on restraining the epidemic from outbreaking. This phenomenon indicates that long-distance travelers play a significant role in spreading the epidemic. Control of epidemic spreading is supposed to focus on carriers of the epidemic moving a long distance.

The epidemic spreading threshold λ_c with respect to the standard deviation σ of the noises is also studied. As it is shown in Fig. 7, the noises lead to smaller threshold λ_c when r_c is smaller than r_s, thus reducing the effectiveness of the IA strategy on restraining the epidemic from outbreaking. Meanwhile, the influence of the noises become smaller when r_c is larger than r_s. In general, the influence of the noises on the epidemic outbreak is indistinctive.

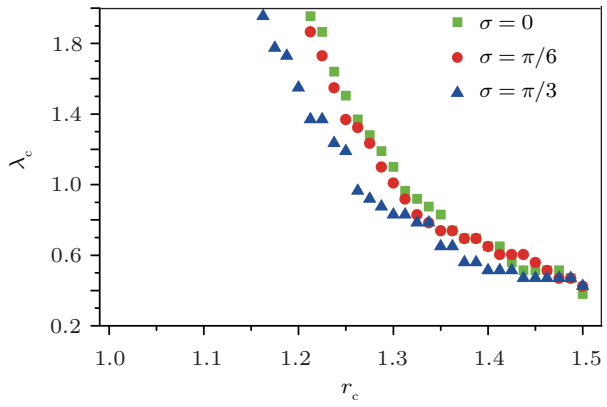


Fig. 7. (color online) Epidemic spreading threshold λ_c with respect to contact radius r_c in the case $\sigma = 0$, $\sigma = \pi/6$, and $\sigma = \pi/3$. The parameters of the model are $N = 200$, $L = 20$, $v = 0.05$, $\rho = 0.5$, $r_s = 1.25$, and $p_{\text{jump}} = 0$. The results are averaged over 10 runs.

3.3. Dynamical evolution process of epidemic spreading

The effects of long-distance jumps on the dynamical evolution process of epidemic spreading are investigated. As shown in Fig. 8, when $p_{\text{jump}} = 0$ and $r_s = 2$, the proportion of infected individuals reaches a peak value and then decreases to zero in simulation. However, once a long-distance jump appears with probability $p_{\text{jump}} = 0.1$, the proportion of infected individuals increases rapidly and the steady-state disease density is rather high, indicating the failure of the IA strategy. In addition, when the IA strategy is not adopted ($r_s = 0$) and $p_{\text{jump}} = 0.1$, the steady-state disease density is a bit larger than that of adopting the IA strategy ($r_s = 2$). This indicates that the IA strategy effectiveness on restraining the epidemic from spreading is heavily reduced when long-distance jumps exist.

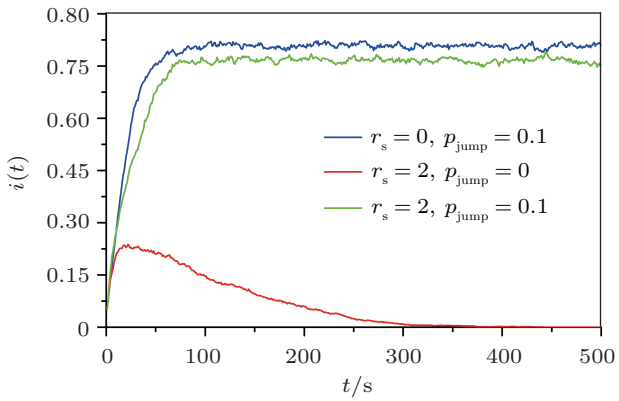


Fig. 8. (color online) Dynamical evolutions of the disease density with respect to simulation steps in the cases of $p_{\text{jump}} = 0$ and $p_{\text{jump}} = 0.1$. The parameters of the model are $N = 200$, $L = 20$, $r_c = 1.4$, $v = 0.05$, $v_{\text{jump}} = 1$, $\rho = 0.5$, $\lambda = 2$, $\mu = 0$, and $\sigma = 0$. The results are averaged over 20 runs.

Figure 9 indicates the influence of the standard deviation σ of the noises on the dynamical evolution process of epidemic spreading. It is found that as σ increases, the peak value of infected individuals becomes larger while the steady-state disease density still decreases approximately to zero in steady-state. This phenomenon coincides with the above results, verifying the effectiveness of the IA strategy on restraining the epidemic from spreading with noises.

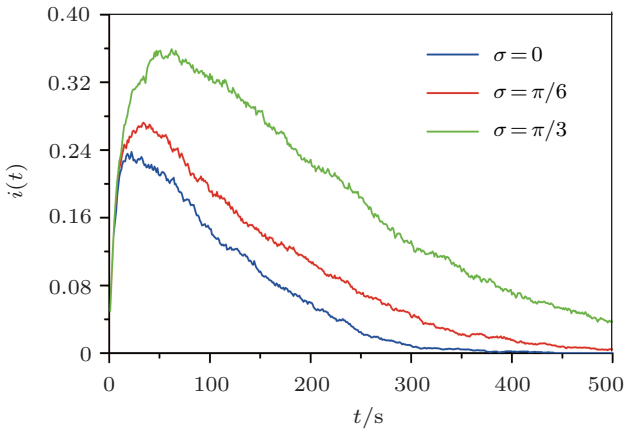


Fig. 9. (color online) Dynamical evolutions of the disease density with respect to simulation steps in three cases of σ. The parameters of the model are $N = 200$, $L = 20$, $r_c = 1.4$, $r_s = 2$, $v = 0.05$, $p_{\text{jump}} = 0$, $\rho = 0.5$, and $\lambda = 2$. The results are averaged over 20 runs.

4. Conclusions

In this paper, we study the model of epidemic spreading on random surfer networks with IA strategy. The long-distance jumps and noises from information transferring process are taken into consideration. Two layers of network are considered: one is the physical contact network through which the epidemic spreads and the other is the directed information network on which the location information of infected individuals is transferred to susceptible individuals. Compared with the models of epidemic spreading on random surfer networks, our model is more logical, as it is more reasonable that susceptible individuals tend to avoid contacting the infected individuals to prevent themselves from being infected. It is found that the IA strategy can restrict the epidemic spreading process significantly when no long-distance jumps exist. However, the IA strategy effectiveness on restraining the epidemic from spreading is highly restricted when long-distance jumps are taken into consideration. This phenomenon warns us that we need to pay high attention to those individuals performing long-distance jumps in order to control epidemic spreading. In addition, it is found that the influence of the noises from transferring process on epidemic spreading is indistinctive.

The model studied in this paper may provide an alternative solution to the control of epidemic spreading. The diversity of individuals with respect to the contact radius r_c and sensing radius r_s is a more challenging research topic in the future.

References

[1] Piet V M, Jasmina O and Robert K 2009 *IEEEACM Transactions on Networking* **7** 1
[2] Wu D Y, Zhao Y P, Zheng M H, Zhou J and Liu Z H 2016 *Chin. Phys. B* **25** 028701
[3] Li K Z, Xu Z P, Zhu G H and Ding Y 2014 *Chin. Phys. B* **23** 118904
[4] Yang H, Tang M, Cai S M and Zhou T 2016 *Acta Phys. Sin.* **65** 058901 (in Chinese)
[5] Ou Y B, Jin X Y, Xia Y X, Jiang L R and Wu D P 2014 *Acta Phys. Sin.* **63** 218902 (in Chinese)
[6] Feng Y, Fan Q L, Ma L and Ding L 2014 *Physica A* **393** 277
[7] Song Y R, Jiang G P and Gong Y W 2013 *Chin. Phys. B* **22** 040205
[8] Hu Z L, Liu J G and Ren Z M 2013 *Acta Phys. Sin.* **62** 218901 (in Chinese)
[9] Liu Z Z, Wang X Y and Wang M J 2012 *Chin. Phys. B* **21** 078901
[10] Huang Y H, Ding L and Feng Y 2016 *Physica A* **444** 1041
[11] Li K Z, Yu H, Zeng Z R, Ding Y and Ma Z J 2015 *Commun. Nonlinear Sci. Numer. Simul.* **22** 596
[12] Pan Q H, Liu R and He M F 2014 *Physica A* **399** 157
[13] Han X P, Zhao Z D, Tarik H and Wang B H 2014 *Commun. Nonlinear Sci. Numer. Simul.* **19** 1301
[14] Zhou J and Chung N N 2012 *Phys. Rev. E* **86** 026115
[15] Arturo B, Luigi F, Mattia F and Alessandro Rizzo 2014 *Phys. Rev. E* **90** 042813
[16] Arturo B, Agnese D S, Luigi F, Mattia F and Vito L 2010 *Int. J. Bifur. Chaos* **20** 765
[17] Liu W P, Liu C, Yang Z, Liu X Y, Zhang Y H and Wei Z X 2016 *Commun. Nonlinear Sci. Numer. Simul.* **37** 249
[18] Wu A C and Wang Y H 2012 *Eur. Phys. J. B* **85** 280
[19] M C G and H J H 2004 *Physica A* **340** 741
[20] Mattia F, Arturo B, Alessandro R, Luigi F and Stefano B 2006 *Phys. Rev. E* **74** 036110
[21] Zhou J and Liu Z H 2009 *Physica A* **388** 1228
[22] Wang Y, Deepayan C, Wang C X and Christos F 2003 *Proceedings of the 22nd International Symposium on Reliable Distributed Systems*, pp. 25–34